Periodic Loading and Selective Undercut Etching for High-Impedance Traveling-Wave Electroabsorption Modulators

Matthew M. Dummer[1], Jonathan Klamkin[1], Erik J. Norberg[1], James W. Raring[2], Anna Tauke-Pedretti[3], and Larry. A. Coldren[1]

[1]Department of Electrical and Computer Engineering, University of California, Santa Barbara, CA 93106
[2] Sandia National Laboratories, Abuquerque, NM 87185 USA
[3]Air Force Research Laboratory, Kirtland AFB, Albuquerque, NM 87117
dummer@ece.ucsb.edu

Abstract: For the first time, selective undercut etching and periodically loaded electrodes are combined to improve impedance and velocity matching for traveling-wave electroabsorption modulators. These devices are fabricated in a platform compatible with widely tunable lasers.

OCIS codes: (250.7360) Waveguide modulators. (230.7020) Traveling-wave devices

1. Introduction

Indium Phosphide based electroabsorption modulators (EAMs) offer a compact solution for efficient, high-speed modulation of optical signals. The utilization of traveling wave (TW) electrodes for EAMs has led to significantly increased bandwidths compared to traditional lumped-element type devices. However, one drawback of TW-EAMs is the low characteristic impedance of the transmission line compared with 50 Ω electrical drivers, due to the high capacitive loading of the p-n junction. This high capacitance also results in slow-wave mode propagation [1] of the electrical signal, which limits the maximum interaction length between the electrical and optical waves. Recently, several methods have been reported for reducing the capacitance per unit length of TW-EAMs including periodic transmission line loading [2], as well as selective undercutting of the active region [3]. For the first time, we have simultaneously utilized both of these techniques to develop high–impedance TW-EAMs which are compatible for integration with sampled-grating (SG) DBR lasers. These TW-EAMs exhibit twice the characteristic impedance compared with previous designs as well as significantly improved return loss and velocity matching. An average impedance of 40 Ω and open eye diagrams at 40 Gb/s with a 1.6 V drive are demonstrated.

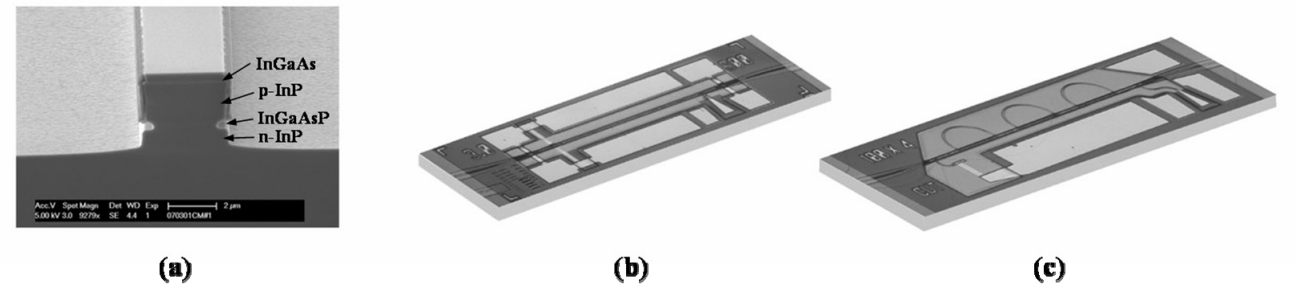

Fig. 1 (a) SEM cross section of undercut EAM structure. (b) Continuously loaded TW-EAM design with integrated termination. (c) Periodically loaded TW-EAM design with integrated termination.

2. Design and Fabrication

The TW-EAM material design was based on the dual quantum well (DQW) epitaxial layer structure for SG-DBR laser integration [4]. These modulators were designed as a proof of concept and, although no lasers have yet been integrated, the entire fabrication process is completely compatible with integrated transmitters. The devices were fabricated on a conducting substrate with a 350 nm InGaAsP waveguide layer, containing 10 quantum wells, between upper and lower InP cladding layers. The photoluminescence peak of the multi-quantum-well stack was 1465 nm. A cross section of the waveguide structure is shown in Fig. 1 (a). The deeply-etched ridge was fabricated first by a combination of dry and wet etching to stop at the quaternary layer. A sidewall mask of SiN was then formed on the upper cladding before dry etching the ridge through the waveguide and lower cladding layer. The waveguide was undercut using a selective wet etch of sulfuric acid and peroxide to reduce the quaternary width from

978-1-55752-855-1/08/$25.00 ©2008 IEEE

3.5 μm to 1.9 μm. The sidewall mask was essential to preserve the p^+-InGaAs contact layer during the selective wet etch. The modulator ridges were buried with a low-k dielectric, Benzocyclobutene, before metallization.

EAMs fabricated with continuously loaded and periodically loaded transmission lines are presented in Fig. 1 (b) and (c), respectively. These devices make use of an on-chip NiCr resistor followed by a DC-blocking capacitor to terminate the traveling wave electrode. The resistor was designed to match the impedance of the TW electrode to prevent electrical reflections. EAMs with coplanar waveguides terminating both sides were also fabricated to allow for two-port S-parameter characterization. The active optical length for both the continuous and periodic TW-EAMs was 400 μm. The periodic electrode was separated into four EAM segments connected by high impedance microstrip lines. Of the total electrode length, only 25% was capacitively loaded, and the path lengths of the unloaded optical and electrical segments were designed to match the propagation distance of the two velocity-mismatched waves.

3. S-Parameter Characterization

We have measured and compared three modulator structures: (1) the continuously loaded TW-EAM with a deeply etched ridge, (2) the continuously loaded TW-EAM with an undercut active region and (3) the periodically loaded design, also with the selective undercut etch. The electrical properties of the different EAM designs were examined by two-port S-Parameter measurements using an HP 8510C network analyzer. The magnitudes of the S-parameter measurements are shown in Fig. 2 (a) at -2.5 V bias. Both undercut designs demonstrate significant improvement over design (1) in both electrical bandwidth and reflected power. The S_{11} measurement shows the return loss of the periodic TW-EAM is well below -10 dB up to 20 GHz, demonstrating better impedance matching to the 50 Ohm electrical drive.

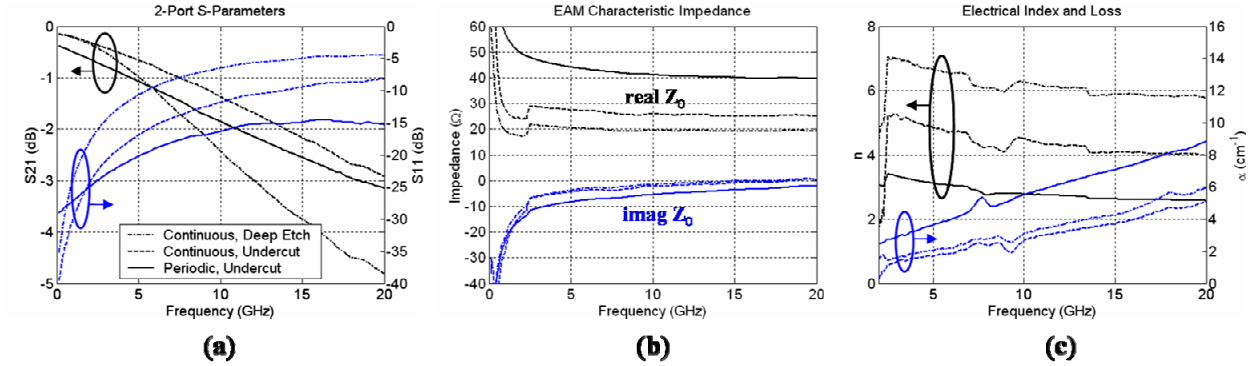

Fig. 2 (a) Two-port electrical S-parameter measurements, (b) Characteristic impedance vs. frequency, and (c) microwave index and attenuation of the three TW-EAM designs at -2.5 V DC bias.

From the S-Parameter measurements we have extracted the transmission line properties of the three structures using the ABCD matrix method [5]. Figure 2 (b) and (c) show the average characteristic impedance as well as microwave index and loss for the different TW-EAMs. The undercut alone increases the impedance of the transmission line from 20 to 26 Ω, and with the addition of the periodic electrode an average impedance of 40 Ω is achieved. The undercut etch also reduces the electrical effective index from 6 to 4, which closely matches the optical group velocity for this waveguide structure. The average electrical index of the periodic electrode is further reduced to nearly 3. This shows good agreement with design simulations which allow for the optical and electrical propagation distances to be matched along the entire device length. For comparison, the microwave loss values of the periodic device are normalized to reflect the loss per active optical length. The loss of the periodic TW-EAM is higher due to the extra 1.2 mm of passive electrode length.

4. Optical Measurements

Optical measurements of the devices have been performed using an external tunable laser source and lensed fibers to couple the light at both facets. Because they are intended to be integrated with a laser, there was no effort to make the EAMs polarization independent so it was necessary to optimize the polarization of the input light for maximum modulation efficiency in these measurements. Small signal electrical to optical (E-O) measurements were made to compare the optical bandwidth of the three TW-EAM designs and to measure the traveling wave effects. Figure 3

(a) shows the normalized frequency response of the three EAMs at -3.0 V bias up to 50 GHz. The values of the on-chip terminations for the continuous and periodic TW-EAMs were 26 Ω and 38 Ω, respectively. The 3-dB bandwidths of the deep-etched, undercut, and periodic designs were 23 GHz, 40 GHz, and 30 GHz, which clearly demonstrates the benefit of the selective undercut etch. The 25% reduction in the bandwidth of the periodic structure is due to the higher microwave loss compared with the continuous, undercut TW-EAM. However, the higher impedance of the device allows for larger voltage swings and less electrical reflections compared with the continuous design. Higher bandwidths can be achieved by terminating the periodic structure with a resistor lower than the characteristic impedance to induce a voltage reflection that results in an enhancement of the frequency response. With 22 Ω terminating the periodic EAM, the bandwidth is increased to 40 GHz.

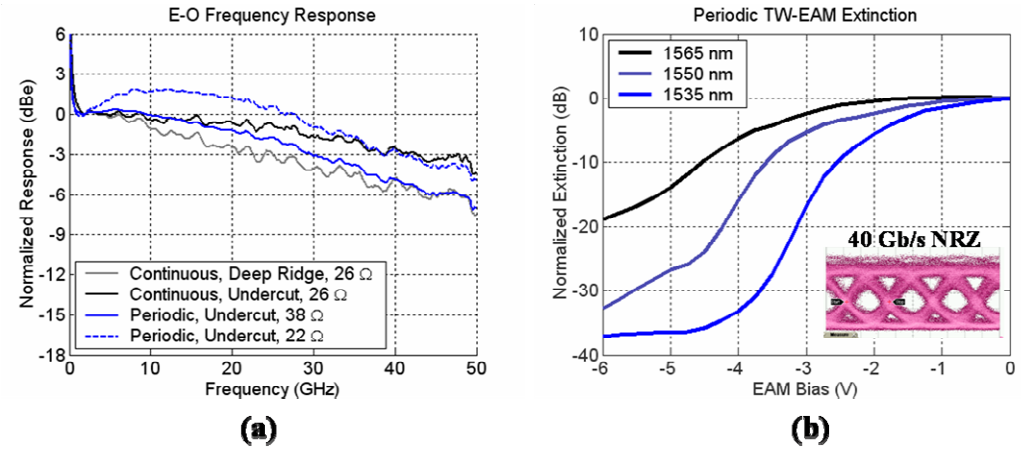

Fig. 3 (a) Optical to electrical frequency response of the different TW-EAM designs for various integrated resistor values. (b) DC extinction vs. wavelength for the periodically loaded TW-EAM. Inset: 40 Gb/s eye diagram.

We have measured DC extinction for the periodic TW-EAM for wavelengths of 1565, 1555, and 1535 nm, shown in Figure 3 (b). The maximum slope efficiencies were 8, 16, and 20 dB/V, respectively. To demonstrate large signal operation of the periodic TW-EAM, we have performed digital data modulation at 40 Gb/s non-return to zero. The device was biased at -3.8 V and terminated with 38 Ω. The inset in Figure 3 (b) shows the observed optical eye diagram at 1550 nm. The dynamic extinction ratio was measured as 6.0 dB for an electrical drive voltage of 1.6 V peak-to-peak.

5. Conclusion

We have demonstrated the first traveling wave EAM to incorporate periodic transmission line loading with selective undercut etching of the active region. This design increases the characteristic impedance by a factor of two, and exhibits excellent velocity matching characteristics. Periodically loading the device improves the return loss by 10 dB at 20 GHz and exhibits an optical bandwidth of 30 GHz for a 400 um long active length. The device demonstrated modulation of digital data up to 40 GB/s with 1.6 V drive. We are currently integrating these EAMs with SG-DBR lasers for tunable transmitters. Future work will focus on reducing the microwave loss to increase the bandwidth, as well as raising the characteristic impedance to 50 Ω to further improve impedance matching.

The authors acknowledge the funding support of the DARPA/MTO/ARL DOD-N program under the LASOR project award number W911NF-04-9-0001.

References

[1] Walker, R.G. *IEEE Journal of Quantum Electronics*, vol. 27, pp 654-667, (1991)
[2] Lewen, R. *et al. Journal of Lightwave Technology,* vol. 22, pp 172-179, (2004)
[3] Chiu, Y. J. *et al. Photonics Technology Letters, IEEE,* vol. 17, pp 2065-2067, (2005)
[4] Sysak, M.N. *et al. Photonics Technology Letters, IEEE* vol. 18, pp 1630-1632, (2006)
[5] Spickermann, R. *et al. Trans. on Microwave Theory and Techniques, IEEE* vol. 42, pp 1918-1924, (2004)